Solid State Science and Technology, Vol. 19, No2 (2011) 25-33
ISSN 0128-7389

SELF-ADHESIVE CARBON GRAINS DERIVED FROM FIBERS OF OIL PALM EMPTY FRUIT BUNCHES FOR BINDERLESS CARBON/CARBON NANOTUBES COMPOSITE ELECTRODES FOR SUPERCAPACITOR APPLICATION

M.M. Ishak[1], M. Deraman[1,*], R. Farma[1,2], Awitdrus[1,2], E. Taer[1,2] and I.A. Talib[1]

[1] School of Applied Physic, Faculty of Science and Technology, Universiti Kebangsaan Malaysia, 43600 Bangi, Selangor, Malaysia

[2]Department of Physics, Faculty of Mathematics and Natural Sciences, University of Riau, 28293 Pekanbaru, Riau, Indonesia

**Corresponding author: madra@ukm.my*

ABSTRACT

Amongst the current trend in the study of carbon composite electrodes is the addition of carbon nano particles, without binding materials, into conventional carbon to produce electrode in order to benefit from both the unique property of the nano particles and the absent of the binder which can improve the specific capacitance of the electrodes. In our study, we produce the binderless carbon/carbon nanotubes composite electrodes for supercapacitor application from the green pellets consist of self-adhesive carbon grain from fibers of oil palm empty fruit bunch and 0, 6 and 8% carbon nanotubes (CNTs), respectively. This paper reports the electrodes properties, i.e., microstructure, electrical conductivity, porosity and electrochemical, based on the characterization using Field Emission Scanning Electron Microscope, four-point-probe, nitrogen adsorption-desorption isotherm, electrochemical impedance spectroscopy and cyclic voltammetry techniques. The results show that supercapacitor cell using the electrodes with 6% CNTs has a better supercapacitive behavior.

Keywords: Self-Adhesive Carbon Grains (SACG); Carbon Nanotubes (CNTs); Electrical Conductivity; Surface Area; Microstructure; Specific Capacitance;

INTRODUCTION

Different types of carbon precursors are available and have been used to produce carbon electrode for supercapacitor application. Large variety of carbon precursor has lead to various types of techniques or approaches in the method of preparation of carbon electrodes. Amongst the popular one is to avoid using binding agent because of the several reason, i.e. it can reduce pores and electrical conductivity of the sample as well as it can simplify the fabrication process. Examples of carbon precursors that can produce binderless carbon electrode are mesophase-based materials [1]. In our study we have used a pre-carbonized fibers of oil palm empty fruit bunches (EFB) as a carbon precursor which can be produced using a procedure described in references [2, 3].

Solid State Science and Technology, Vol. 19, No2 (2011) 25-33
ISSN 0128-7389

Carbon-carbon composites containing multi-walled carbon nanotubes (MWCNTs) have better mechanical and thermal/electrical barrier [4]. The carbon nanotubes (CNTs) with an appropriate quantity in supercapacitor carbon electrodes have higher specific capacitance and electrical conductivity [5], and better electrochemical property [6-7]. An appropriate quantity of MWCNTs in naphthalene-derived synthetic mesophase pitch precursor can also improved the production of the carbon-carbon composite [8]. In our study, we have produced carbon-nanocarbon composites from a mixture of CNTs and a matrix precursor, namely self-adhesive carbon grains (SACG), which was prepared from fibers of oil palm EFB. Characterizations of the activated carbon/CNTs composite produced were carried out using four-point-probe, Field Emission Scanning Electron Microscope (FESEM) and nitrogen adsorption-desorption isotherm techniques. Supercapacitor cells constructed using this composite as electrodes were characterized using electrochemical impedance spectroscopy (EIS) and cyclic voltammetry (CV) techniques. Reports on the characterization and preparation of carbon pellets from SACG and treated SACG are available elsewhere [2-3, 9-13].

EXPERIMENTAL DETAILS

Sample Preparation

The fibers of EFB supplied by Stable-Win Sdn. Bhd. Malaysia, were pre-carbonized for 1 hour and 43 minutes at 280 ^{o}C under vacuum (Furnace CTMSB46) following our previous method [2]. The pre-carbonized fibers of EFB were ground and sieved to obtain SACG powder that pass through a sieve with size 106 µm mesh. The SACG were later mixed with 6 and 8% of CNTs and the mixtures (10 g) were milled for 6 minutes to obtain homogeneous mixtures of SACG and CNTs (Rocklabs Bench Top Ring Mill Model No. C9-D818-075230-100N). The SACG powder without CNT (10 g) was also milled for 12 minutes to ensure both set of samples underwent the same milling process. A press pelletizing machine with a sufficient (196 > kgcm^2) compression force was used to convert 0.75 g of the powder samples inside a mould with a diameter of 20 mm into the green pellet (GPs). A stopper with thickness of 1.4 mm was used to control the pellet thickness. Three replicate samples, label as GP1, GP2 and GP3 were prepared.

The carbonization of the GPs to obtain carbon pellets (CPs) was done using a carbonization furnace (Vulcan Box Furnace 3-1750) under a 1.5 *l* min^{-1} flow of N_2 gas using our previous multi-step heating profile [2]. The carbonization started with a heating rate of 1 ^{o}C per minute from room temperature to 320 ^{o}C, holding at this temperature for 1 h and continued at 3 ^{o}C per minute to 800 ^{o}C. The CO_2 activation on the CPs was carried out at a temperature of 800 ^{o}C for 1 h in a flow of 1.5 *l* min^{-1} CO_2 gas with a heating rate of 5 ^{o}C per minute to produce activated carbon pellets (ACPs).

Characterization

The dimensions (Mitutoyo 193-253) and weight (Mettler Toledo AB204) of the pellets before and after carbonization were measured. The electrical conductivity of the

samples was determined using a four-point-probe technique (Jandel Universal Probe & Keithley Micro-Ohmeter 220). In this study, the voltage (V) and current (I) were recorded and their value were used in the equation (1) [14].

$$\sigma = \frac{I}{2\pi sV} \qquad (1)$$

where, s is the distance between probes (0.7833 mm).
Field Emission Scanning Electron Microscope (FESEM) measurements (Zeiss SUPRA 55VP) were used with a magnification of 1000, 5000 and 50 000 X to study the microstructures and morphology of the fractured surface of ACPs. The nitrogen adsorption-desorption isotherm technique was used to characterize the porosity of the ACPs. The measurements were carried out at 77 K using a BELSORP Mini II instrument. The specific surface area of the samples was determined from the nitrogen adsorption-desorption isotherm data by the standard BET method. The micropore volume was calculated using a t-plot analysis. The mesopore volume was obtained by subtracting the micropore volume from the total pore volume.

The ACPs were polished into a thickness of 0.85 mm and used them as electrodes in a symmetrical supercapacitor cells which contain 1 M H_2SO_4 electrolyte and stainless steel (316) plate (0.5 mm) current collector. The electrochemical behavior of the fabricated supercapacitor cell was investigated using an Impedance Spectrum Analyzer (Solartron 1260) and Potentiostat (Solartron 1287). With a frequency range from 1 x 10^6 to 1 x 10^{-1} Hz and 10 mV voltage amplitude, the impedance data of EIS were recorded in terms of the imaginary impedance (Z") and real impedance (Z') for our cells and a reference commercial cell for comparison. The specific capacitance, C_{sp} of the carbon electrode can be calculated from the EIS data using equation (2) [15].

$$C_{sp} = -\frac{1}{2\pi f \times Z'' \times m} \qquad (2)$$

where *f* is the frequency, Z'' is the imaginary impedance for the cell and m is the mass of the electrode.

The CV data which represent the response of capacitor against potential change between electrodes of the supercapacitor cells was obtained for a potential range from -1 V to 1 V at a scan rate (S) of 5 mVs^{-1} using the same measurement device (Solartron 1287). The specific capacitance, C_{sp} of the carbon electrode can be calculated from the CV data using equation (3) [16].

$$C_{sp} = -\frac{I}{S \times m} \qquad (3)$$

where I is the current, S is the scan rate applied and m is the mass of the electrode.

Solid State Science and Technology, Vol. 19, No2 (2011) 25-33
ISSN 0128-7389

RESULTS AND DISCUSSION

Table 1 shows the weight, dimension and density of the GPs. The data in this table clearly show that the addition of the CNT causes the dimension of the sample to increase and consequently decrease the density of the sample. This indicates that the CNT is lighter in weight compared to that of the SACG.

Table 1: The weight (m), thickness (t), diameter (d), density (ρ) and porosity of the GPs, [A: 0% CNT 100% SACG, B: 6% CNT 94% SACG, C: 8% CNT 92% SACG]

Sample	m (mm)	t (mm)	d (mm)	ρ (g/cm^3)	Porosity (%)
A1	0.7271	1.91	20.08	1.2020	47.0
A2	0.7191	1.90	20.09	1.1938	47.4
A3	0.7233	1.91	20.08	1.1957	47.3
B1	0.7236	1.92	20.14	1.1829	47.8
B2	0.7222	1.93	20.13	1.1756	48.2
B3	0.7248	1.93	20.14	1.1787	48.0
C1	0.7234	1.94	20.16	1.1680	48.5
C2	0.7227	1.94	20.16	1.1669	48.6
C3	0.7244	1.95	20.16	1.1636	48.7

Table 2: The weight (w), thickness (t), diameter (d), density (ρ), conductivity (σ) and porosity of the CPs after carbonization, [A: 0% CNT 100% SACG, B: 6% CNT 94% SACG, C: 8% CNT 92% SACG]

Sample	m (mm)	t (mm)	d (mm)	ρ (g/cm^3)	σ $(\Omega mm)^{-1}$	Porosity (%)
A1	0.2636	1.34	14.25	1.2333	0.4526	45.6
A2	0.2625	1.34	14.25	1.1937	0.4157	45.9
A3	0.2623	1.35	14.24	1.2199	0.4715	45.8
B1	0.2990	1.35	15.00	1.2532	0.8202	44.7
B2	0.2984	1.35	15.01	1.2490	0.7918	44.9
B3	0.2992	1.35	15.00	1.2540	0.8270	44.7
C1	0.3055	1.37	15.63	1.1621	0.7535	48.8
C2	0.3045	1.38	15.63	1.1499	0.7523	49.3
C3	0.3040	1.38	15.64	1.1465	0.7720	49.5

Table 2 shows that the weight of the sample after carbonization is smaller than that before carbonization, due to the weight loss resulted from the decomposition of the volatile components during carbonization. The sample with higher CNTs content seems to loose less weight and have smaller dimensional shrinkage. This is consistent with the condition that only the SACG component is affected by the carbonization, while the CNTs did not decompose and shrink during carbonization.

Solid State Science and Technology, Vol. 19, No2 (2011) 25-33
ISSN 0128-7389

Although the data in Table 2 show a decreasing trend in the weight and dimension of the samples with respect to the CNTs content but the density appears to be higher for the sample with 6% CNTs. A similar trend is exhibited by the data in Table 3. This result seems to suggest that there is an optimum quantity of CNTs to be added in the sample in order to achieve higher density of the sample. In other words, to promote a better densification of the sample during carbonization, excessive quantity of the CNTs in the samples should be avoided.

The electrical conductivity results of the samples after carbonization and after CO_2 activation are shown in Table 2 and Table 3 respectively. The data in the both table clearly show that the sample with 6% CNT have higher electrical conductivity, which is typically consistent with the trend of the density values. Another noticeable trend is that the electrical conductivity of the samples after CO_2 activation is significantly higher than that after carbonization, despite a small different in their density. The contributing factor to this behavior could be the activation time which was longer than the carbonization time.

Table 3: The weight (w), thickness (t), diameter (d), density (ρ), conductivity (σ) and porosity of the ACPs after CO_2 activation

Sample	m (mm)	t (mm)	d (mm)	ρ g/cm^3)	σ (Ω mm)$^{-1}$	Porosity (%)
A1	0.2606	1.30	14.04	1.2946	1.2548	42.9
A2	0.2606	1.30	14.05	1.2928	1.2288	43.0
A3	0.2617	1.31	14.05	1.2883	1.2315	43.2
B1	0.2951	1.34	14.58	1.3189	1.3824	41.9
B2	0.2945	1.34	14.55	1.3216	1.3856	41.7
B3	0.2948	1.34	14.54	1.3248	1.3615	41.6
C1	0.3028	1.37	15.47	1.1757	1.3553	48.2
C2	0.3022	1.37	15.48	1.1719	1.3072	48.3
C3	0.3015	1.36	15.46	1.1808	1.3146	47.6

Figure 1 shows the plot of the nitrogen adsorption-desorption isotherm for the ACPs at 0% CNT and 6% CNT after CO_2 activation. The adsorption capacity of the later sample appears to be decrease which could be due to the occupancy of CNTs within the pores of the samples. The pores parameter value obtained from the data in this figure is shown in Table 4. It is clear from this table that addition of the CNTs slightly affects the pore characteristic of the samples.

Solid State Science and Technology, Vol. 19, No2 (2011) 25-33
ISSN 0128-7389

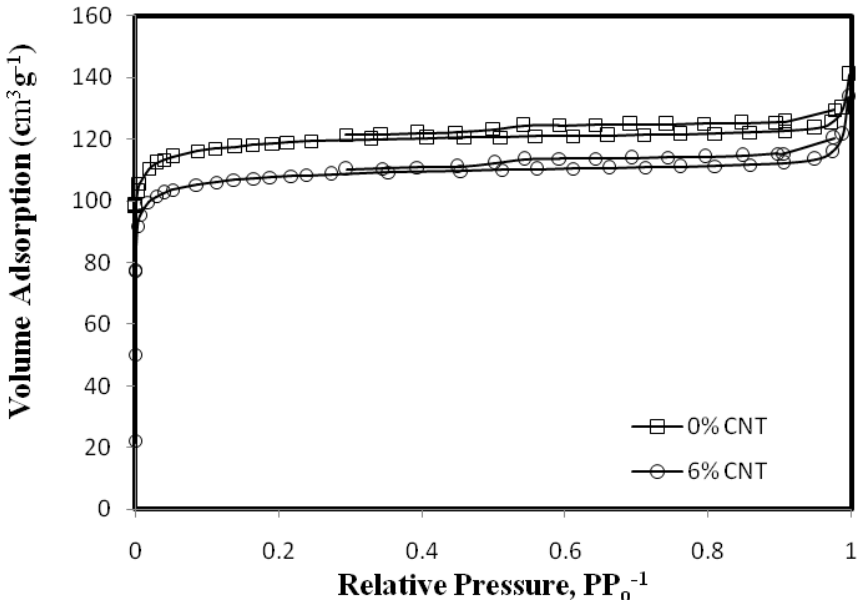

Figure 1: Nitrogen adsorption-desorption isotherm (0 and 6% CNTs)

Table 4: Pore parameters values calculated from nitrogen adsorption-desorption isotherm data

Samples	0%CNT after CO_2	6% CNT after CO_2
S_{BET} [$m^2 g^{-1}$]	456.620	422.460
S_{meso} [$m^2 g^{-1}$]	14.247	14.724
S_{micro} [$m^2 g^{-1}$]	442.373	407.736
V_{total} [$cm^3 g^{-1}$]	0.205	0.193
V_{meso} [$cm^3 g^{-1}$]	0.027	0.032
V_{micro} [$cm^3 g^{-1}$]	0.178	0.161
% Micropore	86.703	83.273
D [nm]	1.796	1.829

The micrographs of the sample obtained from the FESEM technique show that all of the sample were very porous, consisting of macropores, mesopores and micropores. Figure 2 shows the micrographs obtained at the magnification of 50, 000 X for the ACPs at 0%, 6% and 8% CNTs. The micrographs clearly show the presence of the CNTs which occupy pores of the samples.

Solid State Science and Technology, Vol. 19, No2 (2011) 25-33
ISSN 0128-7389

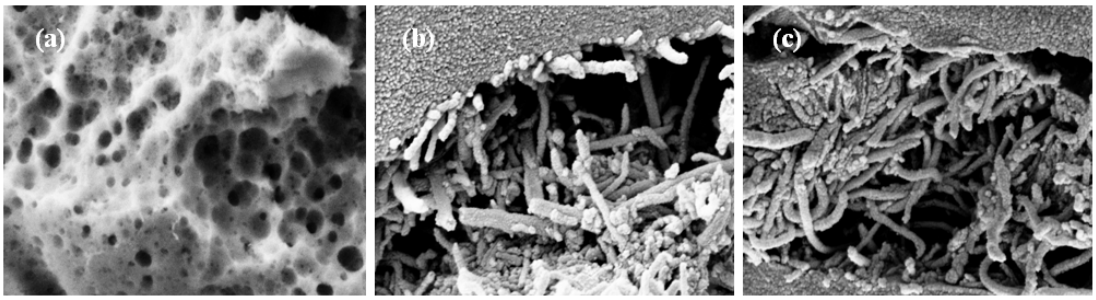

Figure 2: FESEM micrographs with 50 K X magnification for ACPs with 0, 6 and 8% CNTs

Figure 3 shows the EIS spectra for the supercapacitor cell using the ACPs at 0%, 6% and 8% CNTs as electrodes. All of the cells show a typical supercapacitive behavior but the detail of the impedance spectra is different [10]. A common feature of the spectra includes the presence of the Warburg region, semicircle and supercapacitive region. The specific capacitance (C_{sp}), electrode contact resistance of the electrode (R_s), resistance of ion migration in the bulk solution (R_p) and knee frequency (f_k) values determined from these EIS spectra are shown in Table 5, which indicates that the role of the CNTs addition in reducing the R_s and R_p values but does not significantly reduce the value of the specific capacitance.

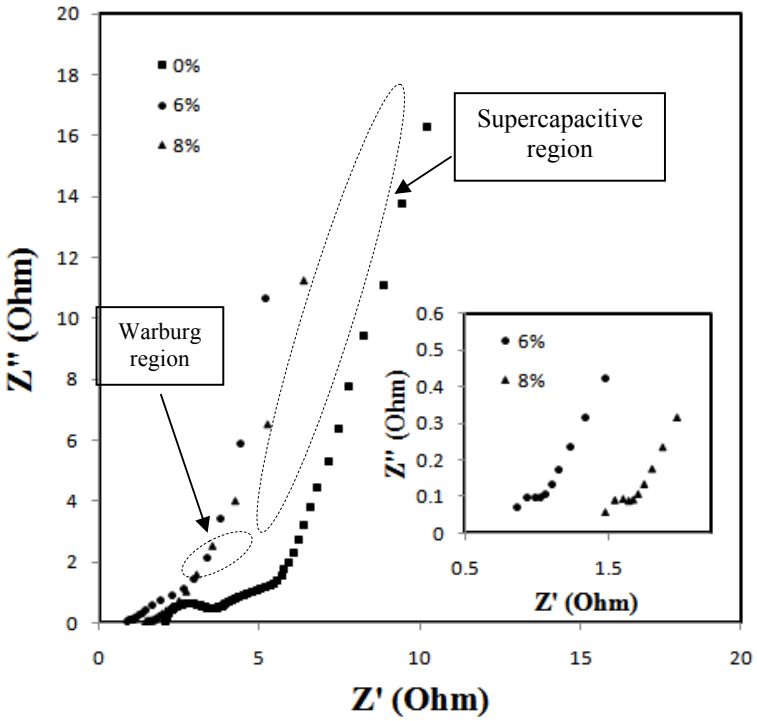

Figure 3: EIS spectra for cells using ACPs (0, 6 and 8% CNTs)

Solid State Science and Technology, Vol. 19, No2 (2011) 25-33
ISSN 0128-7389

Table 5: Parameters values obtain from EIS data

Supercapacitor Cell (CNT %)	C_{sp} (Fg^{-1})	R_s (Ω)	R_p (Ω)	f_k (Hz)
0%	1.4068	2.0447	3.6947	10.000
6%	6.1590	0.8099	1.1232	3.9811
8%	5.1800	1.4230	1.7317	7.9433

Figure 4 shows the CV data for the supercapacitor cell using the ACPs with 0%, 6% and 8% as electrodes, and also for a reference cell. All of the cell show a general typical shape (nearly rectangle pattern) of cyclic voltammogram, but differ in their detail behavior. The cell with 6 % CNTs shows a larger area of rectangle compared to that with 8 % CNTs, indicating that the former cell has a better supercapacitive characteristic. The presence of the CNTs in the samples seems to introduce a pair of redox peaks at certain value of the voltage. These peaks are possibly associated with the influence of the redox reaction [17].

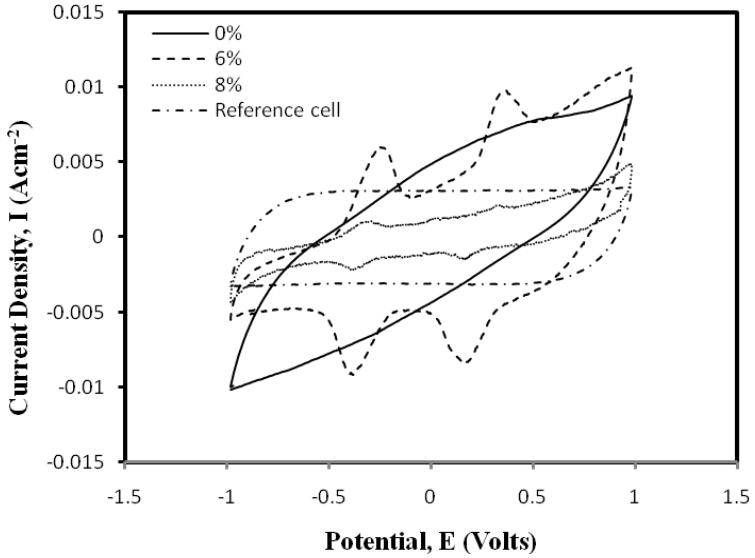

Figure 4: CV curves for cells using ACPs (0, 6 and 8% CNTs)

CONCLUSION

Binderless carbon/carbon nanotubes composite electrodes for supercapacitors have been produced from the green bodies consisting of carbon nanotubes and self-adhesive carbon grain from fibers of oil empty fruit bunches. Results from the FESEM and nitrogen adsorption isotherm techniques showed the porous characteristic of the electrodes, which was slightly affected by the presence of CNTs. This porous behavior contributed to the supercapacitive behavior of the cell produced, with the electrodes of 6% CNT showed better results than the other electrodes containing 0 and 8% CNT.

ACKNOWLEDGEMENT

The authors acknowledge Research University Grant (UKM-GUP-NBT-08-27-107) from Ministry of Higher Education, Malaysia (MOHE) for the project entitled 'Electrodes Supercapacitor from Fibers of EFB', Fundamental Research Grant (UKM-ST-07-FRGS0030-2009) from MOHE for the project entitled 'Study of Interface between Current Collector and Carbon Electrode Based on Biomass and Nanomaterials in Supercapacitor' and also Research University Grant (UKM-OUP-29-145/2011). The assistance of Mr. Saini Sain and other members of Nano-ionic Research are gratefully acknowledged.

REFERENCES

[1] V. Ruiza, C. Blancoa, R. Santamarı´a, J.M. Ramos-Ferna´ ndez, M. Martı´nez-Escandell, A. Sepu´ lveda-Escribano and F. Rodrı´guez-Reinoso, *Carbon,* **47** (2009) 195 –200
[2] M. Deraman, R. Omar and A. G. Harun, *J. Mater.Sci. Lett.* **17** (1998) 2059-2060
[3] M. Deraman, R.Omar, S. Zakaria, I.R. Mustafa, M. Talib, N. Alias and R. Jaafar, *J.Mater. Sci.*, **37** (2002) 3329-3335
[4] Y. Song, S. Li, G. Zhai, J. Shi, Q. Guo and L. Liu, *Mater. Lett.*, **62** (2008) 1902–1904
[5] V. V. N. Obreja, *Phys. E.* **40** (2008) 2596–2605
[6] C. Portet, P. L. Taberna, P. Simon and E. Flahaut, *J. Power Sources,* **139** (2005) 371–378.
[7] P. L. Taberna, G. Chevallier, P. Simon, D. Ple´e and T. Aubert, *Mater. Res. Bull.* **41** (2006) 478–484
[8] X. Qing, L. Liu and Q. Guo, *Mater. Lett.* **59** (2005) 3062-3065
[9] Awitdrus, M. Deraman, I. A. Talib, R. Omar, M. H. Jumali, E. Taer and M. M. Saman, *Sains Malaysiana.* **39** (1) (2010 83–86
[10] E. Taer, M. Deraman, I.A. Talib, A.A. Umar, M. Oyama and R.M. Yunus, *Curr. Appl. Phys.* **10 (4)** (2010) 1071-1075
[11] M. Deraman, R. Omar, S. Zakaria, M. Talib, I. R. Mustapa, A. Azmi and A.A. Aziz, *Adv. Polym. Technol.* **23 (1)** (2004) 51-58
[12] M. Deraman, A. A. Aziz, M. Mokhtar and R. Omar, *Phys. J. IPS.* **A6** (2002) 0514 1-4
[13] M. Deraman, S. Zakaria, R. Omar and A. A. Aziz, *Jpn. J. Appl. Phys.* **39** (12A) (2000) 1236-L1238
[14] Blythe and A.R. *Electrical properties of polymers,* (Cambridge University Press, Cambrige, England 1980)
[15] J.G. Lee, J.Y. K and S.H. Kim, *J. Power Sources* **160** (2006) 1495–1500
[16] V. Komenko, E. Frackowiak, F. Béguin, *Electrochim. Acta.* **50** (2005) 2499-2506
[17] B. E. Conway, Electrochemical Supercapacitors, *Scientific Fundamentals and Technological Applications,* (Kluwer Academic/Plenum Publishers, New York, 1999)